LAWRENCE
LIVERMORE
NATIONAL
LABORATORY

LLNL-JRNL-409386

Disturbance of isotope systematics in meteorites during shock and thermal metamorphism and implications for shergottite chronology

A. M. Gaffney, L. E. Borg, Y. Asmerom

December 15, 2008

Meteoritics and Planetary Science

Disclaimer

Disturbance of isotope systematics in meteorites during shock and thermal metamorphism and implications for shergottite chronology

By: Amy M. Gaffney[1*], Lars E. Borg[1] and Yemane Asmerom[2]

December 10, 2008

1. Lawrence Livermore National Laboratory, Physical and Life Sciences, Institute of Geophysics and Planetary Physics, Livermore, CA 94550

2. Department of Earth and Planetary Sciences, University of New Mexico, Albuquerque, NM, 87131

*corresponding author; gaffney1@llnl.gov; 925-422-4396

Abstract

Shock and thermal metamorphism of meteorites from differentiated bodies such as the Moon and Mars have the potential to disturb chronometric information contained in these meteorites. In order to understand the impact-related mechanisms and extent of disturbance to isochrons, we undertook experiments to shock and heat samples of 10017, a 3.6 billion year old lunar basalt. One sub-sample was shocked to 55 GPa, a second sub-sample was heated to 1000˚ C for one week, and a third sub-sample was maintained as a control sample. Of the isotope systems analyzed, the Sm-Nd system was the least disturbed by shock or heat, followed by the Rb-Sr system. Ages represented by the ^{238}U-^{206}Pb isotope system were degraded by shock and destroyed with heating. In no case did either shock or heating alone result in rotated or reset isochrons that represent a spurious age. In some cases the true crystallization age of the sample was preserved, and in other cases age information was degraded or destroyed. Although our results show that neither shock nor thermal metamorphism alone can account for the discordant ages represented by different isotope systems in martian meteorites, we postulate that shock metamorphism may render a meteorite more susceptible than unshocked material to subsequent disturbance during impact-related heating or aqueous alteration on Mars or Earth. The combination of these processes may result in the disparate chronometric information preserved in some meteorites.

Introduction

A principal goal of meteorite studies is to establish the geologic history of the meteorite's parent body. Meteorites from differentiated bodies, such as Mars or the Moon, potentially record information on the timing and duration of geologic processes including planetary differentiation, volcanism and hydrothermal activity. Identification of such events is based primarily on isotopic analyses that establish the chronology of events and constrain the compositional characteristics of the source from which an individual meteorite is derived. The most commonly used method for determining the age of a meteorite involves measuring parent-daughter radionuclide pairs in various mineral fractions separated from the meteorite to determine both a mineral isochron and the initial isotopic composition of the sample. A requirement of this technique is that the isotope systematics of the meteorite have remained undisturbed since the minerals formed. However, in the case of some martian and lunar meteorites, the isotopic compositions of various mineral and whole rock fractions either fail to yield well-defined isochrons, or yield isochrons in different isotope systems that give discordant ages, indicating that these meteorites have experienced some disturbance since the time of crystallization (e.g., Lugmair et al., 1976; Papanastassiou and Wasserburg, 1976; Shih et al., 1982; Chen and Wasserburg, 1986; Borg et al., 1997). The discordant ages in martian meteorites have led to fundamentally contrasting interpretations of the timing of martian magmatism. Among the shergottites, there are individual samples that yield internally well-defined isochrons with highly discordant ages. Specifically, Rb-Sr and Sm-Nd isotope systems yield concordant ages that have been interpreted to represent crystallization at relatively young ages (165-575

Ma; Shih et al., 1982; Borg et al., 2001; Nyquist et al., 2001; Morikawa et al., 2001; Brandon et al., 2004; Symes et al., 2005), whereas the ^{206}Pb-^{207}Pb isotope system has been interpreted to reflect crystallization at a relatively ancient age (~4 Ga; Bouvier et al., 2005). Furthermore, all isotopic systems (including Rb-Sr, Sm-Nd, Lu-Hf, U-Pb and ^{206}Pb-^{207}Pb) show some non-linear behavior on isochron diagrams indicating that, in some samples, they are disturbed by post-crystallization processes. Thus, chronologic studies of these meteorites appears to be hampered by post-crystallization disturbance that modified or destroyed chronologic information in the sample. Deciphering the chronology of the martian meteorites requires separating the effects of secondary disturbance from the isotopic record of primary crystallization.

There are a number of processes that could potentially disturb isotope chronometers in the martian meteorites. Possibilities include shock and thermal metamorphism resulting from impact processes, alteration (via reactions that decompose the minerals to form new ones) and contamination (via addition of extraneous components to the rock). Petrologic and geochemical evidence in meteorites indicates that alteration and contamination affect many meteorites (e.g., Treiman et al., 1993; Crozaz et al., 2003), whereas every meteorite experiences at least one impact event, related to the ejection of the meteorite from its parent body. The range and extent of disturbance that can result from impact metamorphism and the modification that this can cause to isotope chronometers is not well established. A preliminary study found Rb loss as well as a minor degree of Sm-Nd isochron rotation in an experimentally heated sample (Nyquist et al., 1988; Nyquist et al., 1991), whereas no effect was observed in the Rb-Sr isochron of an experimentally

shocked sample (Nyquist et al., 1987). Thus, to more completely characterize the effects of this ubiquitous process on meteorite chronometry, we have undertaken an experimental study of the effects of impact-related metamorphism on the radiogenic isotope systematics in a basalt. The approach to this study is to determine the response of Sm-Nd, Rb-Sr, U-Pb and ^{206}Pb-^{207}Pb isotope chronometers to shock and heating. The sample selected for this study is a lunar basalt that has been petrographically, geochemically and chronologically well-characterized. A lunar basalt was selected because these basalts are sufficiently old that that they contain variable amounts of radiogenic Sr, Nd and Pb in the mineral fractions, and are essentially free of alteration, thus eliminating this variable as a possible cause of disturbance. This particular sample, 10017, was previously shocked in the course of other experiments, and it is adequately coarse-grained to enable preparation of pure mineral separates. One sub-sample of this basalt was heated in a manner to simulate the effects of post-impact thermal metamorphism, and a second sub-sample was shocked at 55 GPa to simulate the effects of the impact. A third sub-sample was left undisturbed as a control sample. In this paper, we first present detailed results from these experiments. We then apply these results to the case of martian meteorites, and evaluate the likely possible causes of discordant ages reflected by different chronometers in several martian meteorites.

Sample and procedures

Lunar mare basalt 10017,328 is the sample used in this study. Its primary constituents are clinopyroxene (45-55%), plagioclase (24-35%), ilmenite (15-20%) and mesostasis (~8%)

(Schmitt et al., 1970; Beaty and Albee, 1978). Trace phases include cristobalite, tridymite, troilite, apatite, whitlockite, ulvöspinel, and Fe-metal (Papike et al., 1976; Beaty and Albee, 1978). Three sub-samples of 10017 were prepared and analyzed for this study. One sub-sample was experimentally shocked at 55 GPa, by F. Hörz at NASA-Johnson Space Center. A second sub-sample was heated to 1000 ˚C, under vacuum (1 x 10^{-5} torr) for 170 hours. A third sample was left unheated and unshocked, as an experimental control. The high ilmenite content of this sample is unique to lunar basalts, and therefore introduces a compositional variable to this work that is not represented in other planetary basalts such as the martian meteorites. However, the prior shock experiments on this sample made it otherwise ideal for this study.

Because of the high percentage of incompatible element-enriched mesostasis present in this sample, the potential effects of heterogeneous distribution of incompatible elements among the three sub-samples is of concern. To ensure that the sub-samples had starting compositions as similar as possible, each sub-sample was made as large as reasonable, given the total amount of starting sample available, and the experimental techniques to be employed. Subsequently, all three sub-samples were processed with the same initial sample preparation and mineral separation procedures, so that the resulting mineral fractions would be directly comparable among the three sub-samples (Fig. 1).

The specific mineral separation techniques employed were chosen because they mimic those used to date basaltic meteorites from Mars, the Moon and smaller differentiated bodies. Each sample was crushed with a sapphire mortar and pestle, and sieved to

separate the 74-150 μm grain size fraction. These fractions were passed through a Frantz isodynamic magnetic separator to isolate plagioclase-rich, pyroxene-rich and ilmenite-rich mineral separates. For the heated and control samples, purified plagioclase and pyroxene mineral separates were generated from the magnetic fractions by hand-picking. Portions of the mineral separates rejected during hand-picking are designated with the suffix '-rej'. The ilmenite-rich magnetic separates were not further purified by hand-picking. The ilmenite-rich fractions also contain a large proportion of mesostasis. There was insufficient material in the shocked sample magnetic separates to further purify with hand-picking. Separate whole rock fractions were obtained from homogenized powders of each of the three samples.

All of the mineral and whole rock fractions were washed in 0.5 N acetic acid, for 10 minutes in an ultrasonic bath, and rinsed with quartz-distilled water. These wash and rinse solutions were discarded. With the exception of the pyroxene-reject, plagioclase-reject and ilmenite-rich fractions, all of the mineral and whole-rock fractions were leached in 2 N HCl, for 10 minutes, in an ultrasonic bath at room temperature. After the leachates were decanted from the solid fractions and reserved for analysis, the fractions were rinsed with quartz-distilled water. The water rinse for each fraction was combined with the corresponding HCl leachate, and these were processed and analyzed along with the residue mineral fractions. Fractions that have been leached are designated with the suffix '(R)', and leachates are designated with the suffix '(L)'. In total, there are nine analyzed fractions for each of the heated and control samples, and seven analyzed fractions for the shocked sample.

The mineral, whole rock and leachate fractions were spiked with mixed ^{87}Rb-^{84}Sr, ^{149}Sm-^{150}Nd and ^{233}U-^{236}U-^{205}Pb tracers, and digested with a combination of HF, HCl and HNO_3. Sequential separations of U, Pb, Rb, Sr, Sm and Nd follow the procedures described by Borg et al. (2005). Isotope ratios were measured using the VG Sector 54 thermal ionization mass spectrometer at University of New Mexico. Data for the shocked and heated samples are reported in Tables 1-3.

Isotope systematics of the 10017 control sample

The Sm-Nd, Rb-Sr and U-Pb isotope data for the unshocked, unheated sample of 10017 are reported and discussed in detail by Gaffney et al. (2007). The relevant results are summarized here. The Rb-Sr, Sm-Nd and ^{238}U-^{206}Pb isotope systems record concordant ages for 10017. The ages preserved by these systems are, respectively, 3678 ± 69 Ma, 3633 ± 57 Ma, and 3616 ± 98 Ma, with initial isotopic compositions of $^{87}Sr/^{86}Sr_i$ = 0.69941 ± 0.00007, ε_{Ndi} = +3.2 ± 0.4 and $^{206}Pb/^{204}Pb_i$ = 31 ± 11. The ^{235}U-^{207}Pb isotope system yields a concordant age of 3800 ± 120 Ma. The ^{206}Pb-^{207}Pb isotope system does not yield a coherent age. Gaffney et al. (2007) attribute this apparent disturbance of ^{207}Pb to contamination of glassy mesostasis in 10017 with highly radiogenic Pb derived from the lunar surface. The Sm-Nd, Rb-Sr, ^{238}U-^{206}Pb and ^{206}Pb/-^{207}Pb/ diagrams for the control sample are shown in Figures 2-5.

Sm-Nd isotope results and observations

In the shocked sub-sample of 10017, all of the analyzed fractions, with the exception of Plag(L), fall within uncertainty of the control sample isochron (Fig. 2b). The Nd isotopic analysis for the shocked Px(R) mineral separate failed, so a complete set of Sm-Nd data for this sample is not available. The recombined shocked WR (R + L) fraction lies on the control isochron, but the recombined shocked Plag (R + L) fraction falls slightly to the left of the control isochron. The values for these 'recombined' points were determined by mathematical calculation from the isotopic and elemental compositions of the (R) and (L) fractions for each fraction type (WR, Plag, etc…). The age calculated from the three mineral and whole rock fractions (Plag(R), Ilm and WR(R)) yields an age of 3650 ± 190 Ma, with an initial ε_{Nd} of +2.77 ± 0.64 (Fletcher and Rosman, 1982; Table 4). The large uncertainty associated with this age is in part due to the small spread in $^{147}Sm/^{144}Nd$ values among the fractions. In the control sample, the Px(R) fraction has the highest $^{147}Sm/^{144}Nd$ ratio, and this helps to constrain the age and initial of that sample. However, an analogous data point does not exist for this sample. The reconstructed WR (R + L), Plag (R + L) and Ilm (unleached) fractions for the shocked sample are not co-linear and therefore yield no meaningful age information.

Nyquist et al. (1988) present Sm-Nd isotopic results for density and magnetic separates of a sample of 10017 shocked at 35 GPa and a corresponding control sample. However, their data show a much smaller range of $^{147}Sm/^{144}Nd$ ratios than is evident in our shocked and control samples. This most likely reflects the different mineral separation procedures used in the two studies. The small range of $^{147}Sm/^{144}Nd$ ratios in the Nyquist et al. (1988)

study precludes the calculation of a precise Sm-Nd isochron. Furthermore, small variations in the compositions of these fractions translate into large variations in calculated isochrons. However, the fractions analyzed are shifted off the control isochron, reflecting a difference in the Sm/Nd ratios of the shocked fraction of up to ~3%. The disturbance is greatest in the most mesostasis-rich fractions, indicating a greater susceptibility to disturbance of glassy mesostasis.

In the heated sample, disturbance is most evident in the leachate fractions and the WR(R) fraction. The three leachate fractions fall above the control isochron, indicating either Sm-Nd fractionation during leaching or preferential incorporation of radiogenic Nd, mobilized from crystal lattice sites damaged by radioactive decay, in the leachates. However, neither of these possible processes appears to have had a significant effect on the position of the corresponding Plag(R) or Px(R) fractions relative to the isochron. In contrast, the WR(R) fraction falls below the control isochron. However, the recombined WR(R) + WR(L) fraction falls directly on the control isochron, indicating that whole rock remained a closed system through the heating event. All of the mineral fractions fall on the reference isochron, and yield a concordant age of 3647 ± 53 Ma and an initial ε_{Nd} of + 2.38 ± 0.37. The calculated age including the WR(R) fraction has a much larger uncertainty: 3521 ± 520 Ma. The recombined fractions (R + L + rej) all fall on the isochron, and preserve a concordant crystallization age, 3632 ± 120 Ma, and an initial ε_{Nd} of + 2.57 ± 0.45 (Table 4).

Rb-Sr isotope results and observations

The shocked sample does not exhibit substantial disturbance in the Rb-Sr isotope system. The slight displacement of the WR(L) fraction to the left of the control isochron is similar to the slight disturbance evident in this fraction in the control sample. Thus, this reflects some disturbance in the sample not related to the experimental procedures. The one notable difference in comparison to the control sample is that the ilmenite-rich fraction in the shocked sample has a much lower $^{87}Rb/^{86}Sr$ ratio, and a correspondingly lower $^{87}Sr/^{86}Sr$, than the ilmenite-rich fraction in the control sample. This is an expected effect from a smaller proportion of incompatible element-enriched mesostasis in the shocked ilmenite-rich fraction (Gaffney et al., 2007). Furthermore, the ilmenite-rich fractions are the most likely to be heterogeneous because ilmenite is the last major phase to crystallize in the rock, and therefore is closely associated with the mesostasis. The four mineral and whole rock fractions yield an age of 3606 ± 190 Ma, with an initial $^{87}Sr/^{86}Sr$ of 0.69945 ± 0.00029. The recombined mineral fractions + Ilm yield similar results: age = 3609 ± 140 Ma and initial $^{87}Sr/^{86}Sr$ = 0.69946 ± 0.00018. These results are consistent with the results of Nyquist et al. (1987) for a sample of 10017 shocked to 35 GPa, who also found minimal disturbance in the Rb-Sr systematics.

The whole rock fraction in the heated sample shows disturbance. The WR(L) fraction falls far to the left of the control isochron, and the WR(R) fraction falls a small distance to the right of the control isochron, consistent with preferential removal of radiogenic Sr by the HCl leachate or Rb-Sr fractionation during leaching. Although the WR(R) and WR(L) fractions fall to opposite sides of the control isochron, the recombined WR

fraction falls slightly to the left of the control isochron, suggesting that the WR fraction did not remain a closed system during heating. The sense of displacement of the recombined WR fraction relative to the control isochron suggests the loss of a small amount of Rb from the sample, via volatilization during heating. The remainder of the heated fractions, both leachates and residues alike, fall on or very slightly to the left of the control isochron. Although the ilmenite-rich fraction falls on the isochron with the mineral fractions, it has lower $^{87}Rb/^{86}Sr$ and lower $^{87}Sr/^{86}Sr$ than the ilmenite fraction from either the control or shocked samples. This indicates either that mesostasis is heterogeneously distributed among the three samples used in this study, or that heating resulted in loss of a high Rb/Sr, high $^{87}Sr/^{86}Sr$ component from the ilmenite and/or mesostasis. The best age for the heated sample, 3586 ± 140 Ma, is derived from the mineral fractions. This age corresponds to an initial $^{87}Sr/^{86}Sr$ of 0.699540 ± 68, which is within uncertainty of the initial derived from the control isochron. The age calculated using the WR(R) and all mineral fractions is 3293 ± 410 Ma. The younger age reflects the disturbance in the WR(R) fraction. The age determined from the recombined fractions + Ilm likewise yields a large uncertainty: 3758 ± 490 Ma.

U-Pb isotope results and observations

Shock metamorphism disturbed the U-Pb systematics of 10017. With the exception of the WR(L) fraction, all of the measured fractions fall below the ^{238}U-^{206}Pb control isochron, and taken together, the fractions demonstrate much more scatter than is evident in the control sample (Figure 4). Correspondingly, this system does not yield well-defined ages

in the shocked sample. The best age, determined from the Px(R), WR(R) and Ilm fractions, is 3484 ± 630 Ma. The age derived from the four mineral and whole rock fractions is 4123 ± 2700 Ma, and the age derived from all seven fractions is 3575 ± 920 Ma. The age derived from the recombined fractions and ilmenite is 3978 ± 1600. Although these ages show general agreement with the crystallization age calculated for the control sample, the disturbance to the sample results in very large uncertainties. The disturbance is most apparent in the plagioclase residue and leachate fractions, which fall farther below the control isochron than any of the other fractions. Furthermore, the mineral and whole rock fractions in the shocked sample, in particular the WR(R) and Ilm fractions, have much lower U/Pb ratios, and correspondingly less radiogenic $^{206}Pb/^{204}Pb$, than in the control sample. This probably reflects heterogeneous distribution of a high-μ trace phase (mesostasis) among the three sub-samples of 10017.

The mineral fractions from the heated sample show extensive scatter in the ^{238}U-^{206}Pb isochron diagram. The best 'age' that can be determined from these data is 1416 ± 1600 Ma, from all mineral and WR(R) fractions. The majority of the fractions are well outside of analytical uncertainty of the control isochron. The WR(R) fraction lies far to the right of the control isochron, and the remainder of the fractions lie to the left of the control isochron. The only fractions that approach the unshocked isochron are the recombined WR fraction, as well as the Px(R), Px(L) and Plag(L) fractions. The location of the recombined WR (R + L) fraction on the control isochron points to closed system behavior of this sample during heating. However, the recombined plagioclase and pyroxene fractions as well as the ilmenite-rich fraction fall to the left of the isochron.

Although the apparently closed-system whole rock requires the existence of a complimentary fraction that falls to the right of the isochron, such a fraction was not analyzed in this study. Although the analyzed fractions in general show a great degree of scatter from the reference isochron, the recombined Plag and Px fractions are nearly identical in their compositions. This indicates that heating effectively homogenized the Pb isotopic and U/Pb compositions of the bulk plagioclase and pyroxene portions of the sample. This observation is discussed further in the following section. The ^{235}U-^{207}Pb isochron is not plotted or discussed because it demonstrates the same relationships as the ^{238}U-^{206}Pb isochron, but corresponds to a higher degree of uncertainty in the age and initial ^{207}Pb/^{204}Pb values determined for the control isochron.

Pb-Pb observations

Although the ^{238}U-^{206}Pb and ^{235}U-^{207}Pb isotope systems in 10017 preserve ages that are concordant with Rb-Sr and Sm-Nd ages, the ^{206}Pb-^{207}Pb data for the control aliquot of 10017 fail to yield an age that is well-defined and concordant with ages determined by the other isotope systems. Gaffney et al. (2007) interpreted these Pb data as reflecting a minor amount of contamination by ancient, radiogenic Pb derived from the lunar surface, via Pb volatilization and recondensation resulting from impacts. Although this contamination disturbed the ^{206}Pb-^{207}Pb ages, it was not sufficient to disturb the U-Pb isotope systematics. However, any disturbance introduced to the ^{206}Pb-^{207}Pb system by the experimental shock and heating procedures is superimposed on an already-disturbed sample.

The fractions in the shocked sample do not show any systematic effects of disturbance. All of the fractions fall in similar relative positions as in the control sample. However, the overall spread of the data defines a more narrow range than in the control sample. This is attributed to bulk sample heterogeneity, which is also evident in the U-Pb systematics. As in the control sample, the shocked WR(R) fraction is more radiogenic than the Ilm fraction. However, in contrast to the control sample, the recombined WR fraction in the shocked sample is more radiogenic than the Ilm fraction. This is an additional indication of heterogeneous distribution of radiogenic Pb-rich mesostasis among the three 10017 sub-samples.

The most notable effects of heating are observed in the relative positions of the various plagioclase and pyroxene fractions. In the heated sample, the Plag(L) and Px(L) fractions have nearly identical, unradiogenic compositions. In comparison, these two leachates in the control sample have compositions that, though at the unradiogenic end of the array, are nonetheless different by ~50%. Thus, heating appears to have homogenized the leachable component in the bulk plagioclase and pyroxene fractions. This same feature is evident in the ^{238}U-^{206}Pb systematics (Fig. 4c). Homogenization is also evident in the nearly identical compositions of the recombined bulk plagioclase and pyroxene fractions in ^{206}Pb-^{207}Pb as well as ^{206}Pb-^{238}U compositional space. In contrast to the heated sample, the recombined Px fraction in the control sample is considerably more radiogenic than the recombined Plag fraction. These changes in the bulk plagioclase and pyroxene fractions are notable effects of the heating procedure and are the most significant effects

observed in all of the experimental results. As pyroxene and plagioclase are the dominant silicate mineral constituents of this sample, this observation suggests that this level of thermal metamorphism effectively homogenizes U and Pb within the silicate portion of the rock. The Px(R) fraction is the least radiogenic of all the heated mineral or rock fractions. This indicates that leached pyroxene, rather than leached plagioclase, is the most reliable recorder of initial (unradiogenic) Pb in a thermally metamorphosed sample.

Elemental Abundances

Prior to analysis, all whole rock and most mineral fractions were leached in 2 N HCl. This procedure is designed to remove labile, terrestrially derived contamination from the grain surfaces. This leaching step is very important when analyzing meteorites that have undergone a period of residence of unknown duration on Earth's surface. This procedure is also used to remove REE-rich phosphate minerals from martian meteorites and thereby generate compositional spread among mineral fractions for Sm-Nd isochrons. Therefore, although the leaching procedure is not strictly necessary for Apollo lunar samples, we included this step in the experimental procedures to simulate the treatment that a meteorite would receive in the course of geochemical analysis.

The large amounts of Sm and Nd present in the leachates (~55-65 % of the amount originally present in the whole rock) reflects the large proportion of the REE budget housed in phosphate minerals (Figure 6, Table 1). These minerals are easily dissolved in HCl. The slight differences in the amount of REE in the leachates among the three

samples reflects slightly different abundances of phosphate minerals among the three samples or other heterogeneity among the three samples. In general, neither shock nor heat appears to result in a significant effect on the mobility of REE during leaching.

Less than 20% of the total Sr and U, and less than 5% of the total Rb, is removed from the sample during leaching. The shocked sample shows lower mobility of Sr and U, and only slightly higher mobility of Rb, relative to both the control sample and the heated sample. Furthermore, the relative positions of the WR(R) and WR(L) fractions in the shocked sample are the same as in the control sample. Therefore, it is most likely that the apparently lower mobility of Sr and U during leaching of the shocked aliquot is simply a reflection of heterogeneity among the sub-samples. In contrast, although the heated aliquot shows a similar amount of Sr mobility compared to the control sample, the composition of this leachate is considerably different, relative to the isochron as well as the WR(R) fraction, in comparison to the control aliquot. In this case, radiogenic Sr has been preferentially incorporated into the leachate.

The greatest change in element mobilization by the leaching process is of Pb in the heated aliquot. Approximately 30% of the Pb is removed from the control and shocked whole rocks by leaching, whereas nearly 70% of the Pb is removed from the heated whole rock by leaching. In the control and shocked samples, the WR(L) and WR(R) fractions generally fall close to the U-Pb isochron. However, in the heated aliquot, the WR(R) fraction lies far to the right of the reference isochron, and the WR(L) fraction falls far to the left of the reference isochron. This is consistent with extensive loss of

radiogenic Pb from the WR(R) fraction, and incorporation of excess radiogenic Pb in the leachate. Additionally, the leachate remains less radiogenic than the WR(R) fraction, as observed in the other samples (shocked and control). This greatly increased mobilization of Pb in the heated aliquot corresponds to loss of age in formation in the U-Pb isotope system, as well as increased scatter in the Pb-Pb isotope system.

Discussion

General observations

Our experiments investigated two endmember effects of an impact: pure shock at a very high pressure and pure heating at a very high temperature. However, natural examples of terrestrial impact craters show that a large range of temperature and pressure conditions may affect material within a single impact structure. Target material at the center of an impact may experience temperatures and pressures up to 1000˚ C and 60 GPa (shock stage IV, Deutsch and Schärer, 1994); at higher T-P conditions the target rock may be melted or vaporized. Thus the shock pressure of our experiment replicates the near-maximum pressure conditions that a target rock may experience prior to complete melting or vaporization. Thermal metamorphism of country rock can result from contact with an impact melt sheet within the crater, or from heating by a continuous breccia deposit located within and outside of the crater, to a distance two crater radii of the crater rim (Deutsch and Schärer, 1994). Miller and Wagner (1979) used zircon and apatite fission tracks from basement rocks and crystalline blocks in the impact breccia at the Ries

impact crater, Germany, to determine the thermal history associated with this impact structure. From the fission track data, they found that the maximum allowable temperature experienced by basement rocks to be ~550-800˚ C, with a duration of less than one hour. The lowest allowable temperature was ~200˚ C, with a much longer duration of 1000 years. Rates of diffusion and chemical reaction, and therefore potential isochron disturbance, are strongly dependent on the time as well as the temperature to which basement rock is heated in an impact. However, it was not reasonable to attempt an experiment that mimics the duration of thermal events on a long (> year) time scale. In the attempt to maximize the possible extent of disturbance produced in our experiments, we conducted the experiment at a higher temperature than would generally be expected to affect the basement rock in a natural impact setting (1000˚ C), and ran the experiment for a duration that was geologically short, but which was reasonable in a laboratory setting (1 week). Therefore we believe that the results of our heating experiment reproduce an extreme end of the range of possible outcomes of thermal metamorphism resulting from an impact.

There are three primary conclusions that we derive from our experimental results. These conclusions and their implications for meteorite chronology are discussed below.

1) Neither shock nor thermal metamorphism results in rotated or reset isochrons that represent a spurious age. In some cases the true crystallization age of the sample was preserved, and in other cases age information was degraded or destroyed. However, in several cases, uncertainty on calculated ages is reduced by eliminating certain fractions from the age calculation.

2) Of the isotope systems measured in this study, the Sm-Nd system is the most resistant to disturbance, the Rb-Sr system is less resistant to disturbance, and the ^{238}U-^{206}Pb is the least resistant to disturbance. The ^{206}Pb-^{207}Pb system in the control sample did not yield an age; thus it is not possible to evaluate the resiliency of this isotope system. However, the observation that the control sample does not preserve a ^{206}Pb-^{207}Pb age suggests that this isotope system is highly susceptible to disturbance.

3) Mild HCl leaching enhances disturbance in both shocked and heated samples.

Only the heated sample shows a similar sense of disturbance in all three parent-daughter systems measured. In this sample, for each isotope system, the leached whole rock fraction lies below the isochron and the whole rock leachate lies above. Thus, on the scale of the whole rock, thermal metamorphism results in preferential diffusion of the radiogenic daughter isotope to cracks or grain boundaries from where it is preferentially removed by leaching. For the mineral separates, loss of the radiogenic daughter to the leachate in proportions large enough to affect the composition of the leached mineral fraction is not consistently observed, and therefore we infer that radiogenic daughter is lost primarily from trace phases and glass in the incompatible element-enriched mesostasis contained primarily in the whole rock fraction. This radiogenic component is preferentially removed during leaching. It is evident that it is the combination of leaching with heating that generates this disturbance because, in general, the reconstructed whole rock fractions ((R) + (L)) lie on or close to the control isochrons. This is an important observation, because for meteorite samples, leaching is a necessary analytical step designed to remove terrestrial contamination.

The heated sample shows additional disturbance in the ^{238}U-^{206}Pb and ^{206}Pb-^{207}Pb isotope systems. In both of these isochron diagrams, the bulk pyroxene and plagioclase fractions (recombined R + L + rej) have nearly identical compositions, reflecting Pb isotopic and U/Pb homogenization among these constituents (Figs. 4 and 5). These bulk (recombined) fractions also fall above the isochron, indicating that these samples have been affected by additional disturbance as well as homogenization. However, in both isotope systems, hand-picking and leaching generate compositional spread among the (R) and –rej fractions. In contrast, the Plag(L) and Px(L) fractions have nearly identical and unradiogenic compositions that fall on the reference isochron. These observations indicate that while the bulk plagioclase and pyroxene fractions were affected during heating by either loss of U or gain of radiogenic Pb, this disturbance is localized in the residual mineral fractions. The acid-soluble portion of these fractions remained undisturbed, as illustrated by the observation that the leachates remain on the control isochron. The unradiogenic Pb isotopic composition of these leachates further indicates that they may reliably record the initial isotopic composition of the sample, despite the disturbance evident in the other fractions.

One commonly assumed effect of shock or thermal metamorphism is rotation or resetting of isochrons. Complete resetting of an isochron during a shock or thermal event at some time in the past will generate an isochron that records the age of that event. This results from complete isotopic re-equilibration among the mineral phases in the rock and subsequent ingrowth of the daughter isotope to generate an isochron that records the age

of the disturbance event. This has been suggested as a mechanism to explain discordance between Rb-Sr and Sm-Nd isochrons in some martian meteorites (Bogard et al., 1979; Nyquist et al., 1979; Shih et al., 1982; Jagoutz et al., 1986), where the older Sm-Nd age is inferred to represent the age of crystallization and the younger Rb-Sr age is inferred to reflect the age of shock or thermal metamorphism. It has also been postulated that a shock or thermal event may rotate an isochron in such a way that the mineral fractions maintain their linearity, but the slope of the isochron is changed (without complete resetting) to reflect an age younger than the true crystallization age of the sample, but older than the disturbance event. The possibility that this sort of process may affect meteorites is supported by a study that showed a slight degree of clock-wise rotation of a Sm-Nd isochron in an experimentally shocked sample (Nyquist et al., 1988). Experimentally heated samples showed rotation of the Rb-Sr isochron to a much older age than the control sample, and rotation of the Sm-Nd isochron to a younger age (Nyquist et al., 1991). This result requires very specific re-distribution of parent and daughter isotopes among the mineral fractions, while maintaining mass balance, so that linearity among the fractions is preserved and the isochron is not compressed. In this example, the isochron is not completely reset, so it does not reflect the time at which it is disturbed; rather, it represents an age that has no significance in the history of the sample. However, our results do not show any evidence of isochron rotation or resetting, and therefore do not support the suggestion that these are a common effect of shock or thermal metamorphism nor the cause of isochron disturbance in martian meteorites.

Significance of results for martian meteorite chronology

Collectively, martian meteorites record a complex range of chronometric information that has been interpreted as a record of geologic events including crystallization, meteorite impacts, aqueous alteration and ejection of the meteorite from Mars (e.g. Shih et al., 1982; Chen and Wasserburg, 1986; Jones, 1986; Borg et al., 1999). Whereas some martian meteorites yield concordant ages with multiple chronometers (typically Rb-Sr and Sm-Nd), in other meteorites, different isotope systems yield different ages. This discordance is exacerbated in some samples, for which different sub-sets of mineral, whole rock and leachate fractions define different linear arrays in different isotope systems. In spite of these vagaries, a general consensus has emerged that the Rb-Sr and Sm-Nd arrays in the shergottites represent young (< ~575 Ma) crystallization ages for these samples (summarized by Borg and Drake, 2005). However, linear arrays in ^{206}Pb-^{207}Pb isotope space have recently been interpreted as representing an ancient age of crystallization (~4 Ga) for some shergottites (Bouvier et al., 2005; Bouvier et al., 2008). This interpretation requires a mechanism of disturbance that yields young and concordant though erroneous ages in the Rb-Sr, Sm-Nd, Lu-Hf, ^{238}U-^{206}Pb isotope systems, while preserving an ancient and true ^{206}Pb-^{207}Pb crystallization age. Here we discuss how our new results contribute to this ongoing discussion of the ages of the martian meteorites.

The most significant result from this study is that in no case does simple thermal or shock metamorphism, as represented in our experiments, generate a linear array in any isotope system that corresponds to any age other than the crystallization age recorded in the control sample. In other words, shock or thermal metamorphism did not result in reset or

rotated isochrons in any of the isotope systems we investigated. Instead, shock and heating either had no effect, or resulted degradation or destruction of age information. It is therefore highly unlikely that the ages suggested by linear arrays in any of the martian meteorites are the result of one of the two endmember impact effects investigated here.

The question then remains as to the origin of the multiple ages represented by different isotope systems in the martian meteorites. Although our results strongly suggest that neither pure shock nor pure thermal metamorphism can generate the chronometric disturbances observed in these meteorites, other processes related to impacts may be capable of producing these effects. One possibility is that heating a shocked sample may cause isotopic disturbance that is not evident in a sample that has experienced only shock or only heating. A second possibility is that a shocked sample may be more susceptible to chemical disturbance during subsequent aqueous alteration on Mars or Earth. Although our experiments do not address these possibilities directly, other experiments on the properties of shocked materials indicate that these ideas warrant further exploration. Shock produces crystal defects and fractures within silicate material, which then serve as sites for chemical reaction either as diffusion interfaces during heating or through interaction with an aqueous fluid (Boslough, 1991). Aqueous dissolution experiments show that shocked silicate minerals have a higher rate of reaction in an aqueous fluid than the unshocked counterpart (Boslough and Cygan, 1988; Cygan et al., 1989). Shocked feldspar is also much more reactive than unshocked feldspar, as shown by experimental results in which Na in shocked feldspar exchanged completely with K derived from a surrounding melt (Ostertag and Stöffler, 1982).

These experimental results suggest that shocked martian rocks are likewise more susceptible to chemical modification during post-impact heating or aqueous alteration. Therefore, if the isotopic disturbance in martian meteorites is the result of impact metamorphism, it is the combination of shock with either or both heating and aqueous alteration that generates the effects. The Pb isotope systematics in the martian meteorites are more affected by these processes than the Rb-Sr or Sm-Nd isotope systems for two reasons. First, our experiments show that the Pb isotope systems are the most susceptible to disturbance during heat and shock separately, indicating that the combination of heat and shock will cause greater disturbance to these systems than observed in our experiments. Second, Pb concentrations in martian meteorites are very low, whereas they may be higher in terrestrial or martian aqueous solutions, due to the water-solubility of Pb. This, coupled with the enhanced reactivity of the shocked martian rock, may facilitate contamination of the martian rock with foreign Pb. Although the Pb isotope systems show the greatest extent of disturbance, shock also facilitates disturbance to Rb-Sr and Sm-Nd isotope systems. In most samples, these isotope systems record concordant ages that are taken to be the age of crystallization; however, meteorites exist that show disturbance to one or both of these isotope systems, as well. The variables that influence the extent of disturbance to all of these isotope systems include the shock pressure experienced by the meteorite, extent of post-shock heating, concentration of the elements of interest in the meteorite and the composition of and extent of interaction with aqueous fluids on Mars or Earth.

Conclusions

Both thermal and shock metamorphism result in Rb-Sr and Sm-Nd ages that are concordant with control ages, although in general, the ages derived from the metamorphosed samples have larger uncertainties than the ages of the control sample. This indicates that the Rb-Sr and Sm-Nd isotope systems can be disturbed by extensive heating and shock metamorphism. Only a poorly resolved ^{238}U-^{206}Pb age is preserved in the shocked sample, and all ^{238}U-^{206}Pb age information is lost in the heated sample. The Sm-Nd system is the most resistant, the Rb-Sr system is less resistant, and the ^{238}U-^{206}Pb and ^{207}Pb-^{206}Pb systems are the least resistant to disturbance during shock and thermal metamorphism. Although the inference from meteorites, as well as previous experimental work (Nyquist et al., 1998), is that rotation and resetting of isochrons are common results of metamorphism, our experimental data do not confirm either of these effects. No spurious age information appears to be reflected in our results; in some cases the true crystallization age of the sample was preserved, and in other cases age information was degraded or destroyed. For all isotope systems in the heated sample, the leached whole rock fraction falls to the right of the control isochrons. This suggests that one common effect of thermal metamorphism is be preferential diffusion of the radiogenic daughter isotope to grain boundaries, from where is preferentially removed during leaching. Thus, the combination of heating with leaching, a procedure necessary to remove terrestrial contamination from meteorites, introduces disturbance to the whole rock fractions. The apparent gain of radiogenic Pb by the low-μ ($^{238}U/^{204}Pb$) mineral components during

heating indicates that these components may not be reliable indicators of initial Pb isotopic compositions in planetary materials.

Acknowledgements

We thank F. Hörz for providing the shocked sample of 10017. This work was supported by NASA Mars Fundamental Research Program and Cosmochemistry Program. This work utilized the SAO/NASA Astrophysics Data System. A portion of this work was performed under the auspices of the U.S. Department of Energy by Lawrence Livermore National Laboratory under Contract DE-AC52-07NA27344.

Bibliography

Beaty D. W. and Albee A. L. (1978) Comparative petrology and possible genetic relations among the Apollo 11 basalts. *Proc. 9th Lunar and Planet. Sci. Conf.*, 359-463.

Bogard D. D., Husain L., and Nyquist L. E. (1979) Ar-40/Ar-39 age of the Shergotty achondrite and implications for its post-shock thermal history. *Geochimica et Cosmochimica Acta* **43**, 1047-1055.

Borg L. and Drake M. J. (2005) A review of meteorite evidence for the timing of magmatism and of surface or near-surface liquid water on Mars. *Journal of Geophysical Research (Planets)* **110**.

Borg L. E., Connelly J. N., Nyquist L. E., Shih C.-Y., Wiesmann H., and Reese Y. (1999) The age of carbonates in martian meteorite ALH84001. *Science* **286**, 90-94.

Borg L. E., Nyquist L. E., Reese Y., Wiesmann H., Shih C. Y., Ivanova M., Nazarov M. A., and Taylor L. A. (2001) The age of Dhofar 019 and its relationship to the other martian meteorites. *Lunar and Planetary Science Conference* **XXXII**, 1144.

Borg L. E., Edmunson J. E., and Asmerom Y. (2005) Constraints on the U-Pb isotopic systematics of Mars inferred from a combined U-Pb, Rb-Sr, and Sm-Nd isotopic study of the Martian meteorite Zagami. *Geochimica et Cosmochimica Acta* **69**, 5819-5830.

Borg L. E., Nyquist L. E., Taylor L. A., Wiesmann H., and Shih C.-Y. (1997) Constraints on Martian differentiation processes from Rb-Sr and Sm-Nd isotopic analyses of the basaltic shergottite QUE 94201. *Geochimica et Cosmochimica Acta* **61**, 4915-4931.

Boslough M. B. (1991) Shock modification and chemistry and planetary geologic processes. *Annual Review of Earth and Planetary Sciences* **19**, 101-130.

Boslough M. B. and Cygan R. T. (1988) Shock-enhanced dissolution of silicate minerals and chemical weathering on planetary surfaces. *Lunar and Planetary Science Conference*, 443-453.

Bouvier A., Blichert-Toft J., Vervoort J. D., and Albarède F. (2005) The age of SNC meteorites and the antiquity of the Martian surface. *Earth and Planetary Science Letters* **240**, 221-233.

Bouvier A., Vervoort J. D., and Patchett P. J. (2008) The Lu-Hf and Sm-Nd isotopic composition of CHUR: Constraints from unequilibrated chondrites and

implications for the bulk composition of terrestrial planets. *Earth and Planetary Science Letters* **273**, 48-57.

Brandon A. D., Nyquist L. E., Shih C.-Y., and Wiesmann H. (2004) Rb-Sr and Sm-Nd isotope systematics of shergottite NWA 856: crystallization age and implications for alteration of hot desert SNC meteorites. *Lunar and Planetary Science Conference* **XXXV**, 1931.

Chen J. H. and Wasserburg G. J. (1986) Formation ages and evolution of Shergotty and its parent planet from U-Th-Pb systematics. *Geochimica et Cosmochimica Acta* **50**, 955-968.

Crozaz G., Floss C., and Wadhwa M. (2003) Chemical alteration and REE mobilization in meteorites from hot and cold deserts. *Geochimica et Cosmochimica Acta* **67**, 4727-4741.

Cygan R. T., Casey W. H., Boslough M. B., Westrich H. R., Carr M. J., and G. R. Holdren J. (1989) Dissolution kinetics of experimentally shocked materials. *Chemical Geology* **78**, 229-244.

Deutsch A. and Schaerer U. (1994) Dating terrestrial impact events. *Meteoritics* **29**, 301-322.

Fletcher I. R. and Rosman K. J. R. (1982) Precise determination of initial Nd from Sm-Nd isochron data. *Geochimica et Cosmochimica Acta* **46**, 1983-1987.

Gaffney A. M., Borg L. E., and Asmerom Y. (2007) The origin of geochemical diversity of lunar mantle sources inferred from the combined U-Pb, Rb-Sr and Sm-Nd isotope systematics of mare basalt 10017. *Geochimica et Cosmochimica Acta* **71**, 3656-3671.

Jagoutz E. and Wanke H. (1986) SR and Nd isotopic systematics of Shergotty meteorite. *Geochimica et Cosmochimica Acta* **50**, 939-953.

Jones J. H. (1986) A discussion of isotopic systematics and mineral zoning in the shergottites - Evidence for a 180 m.y. igneous crystallization age. *Geochimica et Cosmochimica Acta* **50**, 969-977.

Lugmair G. W., Marti K., Kurtz J. P., and Scheinin N. B. (1976) History and genesis of lunar troctolite 76535 or: How old is old. *Lunar and Planetary Science Conference*, 2009-2033.

Miller D. S. and Wagner G. A. (1979) Age and Intensity of Thermal Events by Fission Track Analysis: the Ries Impact Crater. *Earth and Planetary Science Letters* **43**, 351-358.

Morikawa N., Misawa K., Kondorosi G., Premo W. R., Tatsumoto M., and Nakamura N. (2001) Rb-Sr isotopic systematics of lherzolitic shergottite Yamato-793605. *Antarctic Meteorite Research* **14**, 47-60.

Nyquist L. E., Wooden J., Bansal B., Wiesmann H., McKay G., and Bogard D. D. (1979) Rb-Sr age of the Shergotty achondrite and implications for metamorphic resetting of isochron ages. *Geochimica et Cosmochimica Acta* **43**, 1057-1074.

Nyquist L. E., Hörz F., Wiesmann H., Shih C.-Y., and Bansal B. (1987) Isotopic studies of shergottite chronology: I. effect of shock metamorphism on the Rb-Sr system. *Lunar and Planetary Institute Conference Abstracts*, 732-733.

Nyquist L. E., Bansal B. M., Wiesmann H., Shih C.-Y., and Hoerz F. (1988) Isotopic Studies of Shock Metamorphism: II. Sm-Nd. *Lunar and Planetary Institute Conference Abstracts*, 875.

Nyquist L. E., Bogard D. D., Garrison D. H., Bansal B. M., Wiesmann H., and Shih C.-Y. (1991) Thermal Resetting of Radiometric Ages. I: Experimental Investigation. *Lunar and Planetary Institute Conference Abstracts*, 985.

Nyquist L. E., Reese Y., Wiesmann H., and Shih C.-Y. (2001) Age of EET79001B and implications for shergottite origins. *Lunar and Planetary Science Conference* **XXXII**, 1407.

Ostertag R. and Stoeffler D. (1982) Thermal annealing of experimentally shocked feldspar crystals. *Lunar and Planetary Science Conference*, 457.

Papanastassiou D. A. and Wasserburg G. J. (1976) Rb-Sr age of troctolite 76535. *Lunar and Planetary Science Conference*, 2035-2054.

Papike J. J., Hodges F. N., Bence A. E., Cameron M., and Rhodes J. M. (1976) Mare basalts - Crystal chemistry, mineralogy, and petrology. *Reviews of Geophysics and Space Physics* **14**, 475-540.

Schmitt H. H., Lofgren G., Swann G. A., and Simmons G. (1970) The Apollo 11 samples: Introduction. *Geochimica et Cosmochimica Acta Supplement* **1**, 1.

Shih C.-Y., Wooden J. L., Bansal B. M., Wiesmann H., Nyquist L. E., Bogard D. D., and McKay G. A. (1982) Chronology and petrogenesis of young achondrites, Shergotty, Zagami, and ALHA77005 - Late magmatism on a geologically active planet. *Geochimica et Cosmochimica Acta* **46**, 2323-2344.

Symes S. J. K., Borg L. E., Shearer C. K., and Irving A. J. (2008) The age of the martian meteorite Northwest Africa 1195 and the differentiation history of the shergottites. *Geochimica et Cosmochimica Acta* **72**, 1696-1710.

Treiman A. H., Barrett R. A., and Gooding J. L. (1993) Preterrestrial aqueous alteration of the Lafayette (SNC) meteorite. *Meteoritics* **28**, 86-97.

Figure Captions

Figure 1. Mineral separation schemes for (a) shocked aliquot, and (b) heated aliquot.

Figure 2. Sm-Nd isochron diagrams for (a) control aliquot (Gaffney et al., 2007), (b) shocked aliquot, and (c) heated aliquot. All three panels have the same scale. Ages and initial isotopic compositions are given in Table 4.

Figure 3. Rb-Sr isochron diagrams for (a) control aliquot (Gaffney et al., 2007), (b) shocked aliquot, and (c) heated aliquot. Ages and initial isotopic compositions are given in Table 4.

Figure 4. ^{238}U-^{206}Pb isochron diagrams for (a) control aliquot (Gaffney et al., 2007), (b) shocked aliquot, and (c) heated aliquot. Inset panel in Fig. 4a shows the position of the Ilm and WR(R) fractions relative to the rest of the fractions. Ages and initial isotopic compositions are given in Table 4.

Figure 5. ^{206}U-^{207}Pb isochron diagrams for (a) control aliquot (Gaffney et al., 2007), (b) shocked aliquot, and (c) heated aliquot. Inset panel in Fig. 5a shows the position of the Ilm and WR(R) fractions relative to the rest of the fractions.

Figure 6. Relative element mobility during leaching. Percent of each element in leachate calculated in the basis of the whole rock fraction, as: 100 x (ng element in WR(L))/(ng element in WR(L) + ng element in WR(R)).

Figure 7. Summary diagram of ages determined from Sm-Nd, Rb-Sr and ^{238}U-^{206}Pb isotope systems, for control (Gaffney et al., 2007), shocked and heated samples of 10017.

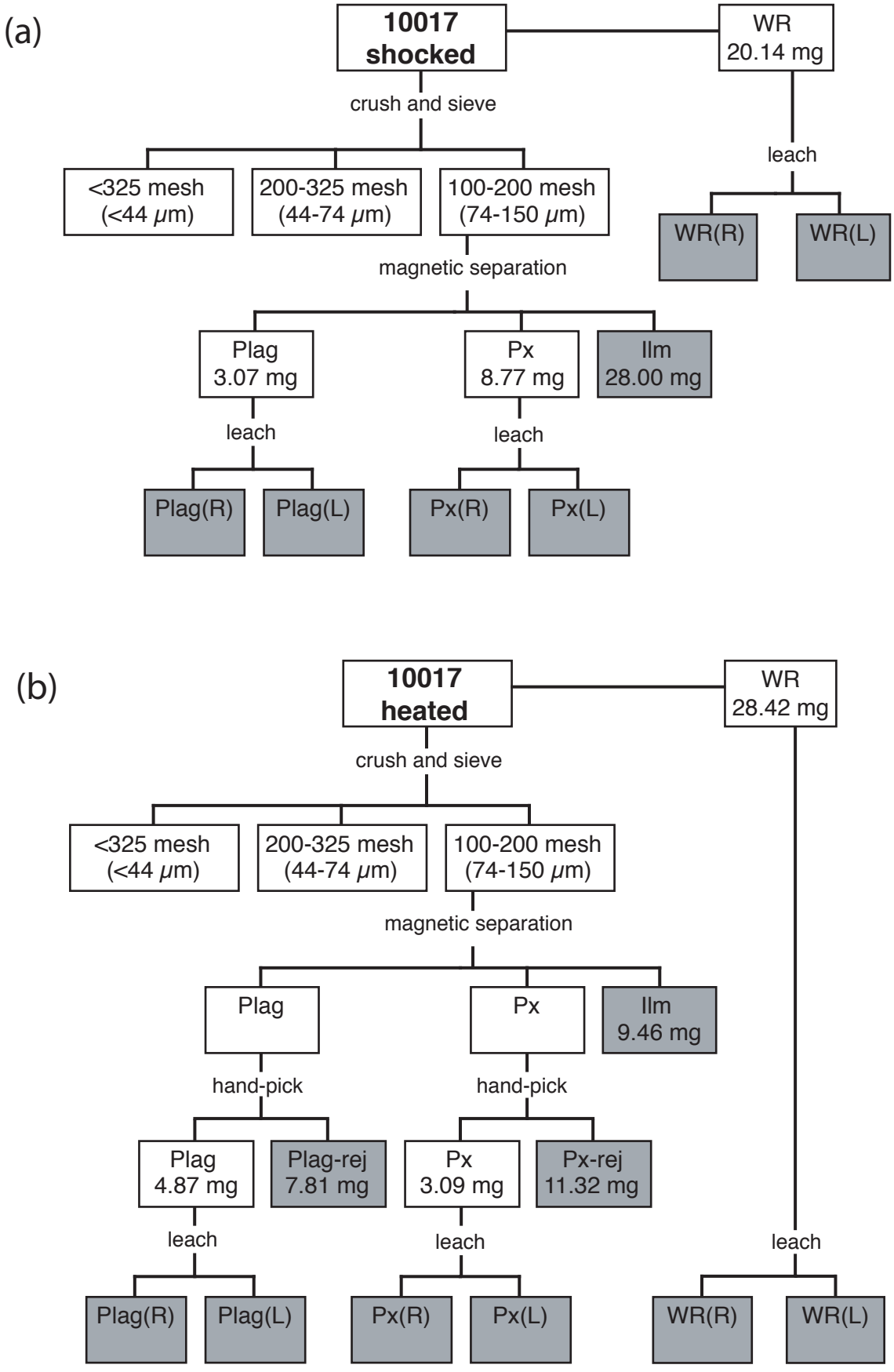
(a)
10017 shocked
WR 20.14 mg
crush and sieve
leach
<325 mesh (<44 μm)
200-325 mesh (44-74 μm)
100-200 mesh (74-150 μm)
WR(R)
WR(L)
magnetic separation
Plag 3.07 mg
Px 8.77 mg
Ilm 28.00 mg
leach
leach
Plag(R)
Plag(L)
Px(R)
Px(L)
(b)
10017 heated
WR 28.42 mg
crush and sieve
<325 mesh (<44 μm)
200-325 mesh (44-74 μm)
100-200 mesh (74-150 μm)
magnetic separation
Plag
Px
Ilm 9.46 mg
hand-pick
hand-pick
Plag 4.87 mg
Plag-rej 7.81 mg
Px 3.09 mg
Px-rej 11.32 mg
leach
leach
leach
Plag(R)
Plag(L)
Px(R)
Px(L)
WR(R)
WR(L)

Figure 1

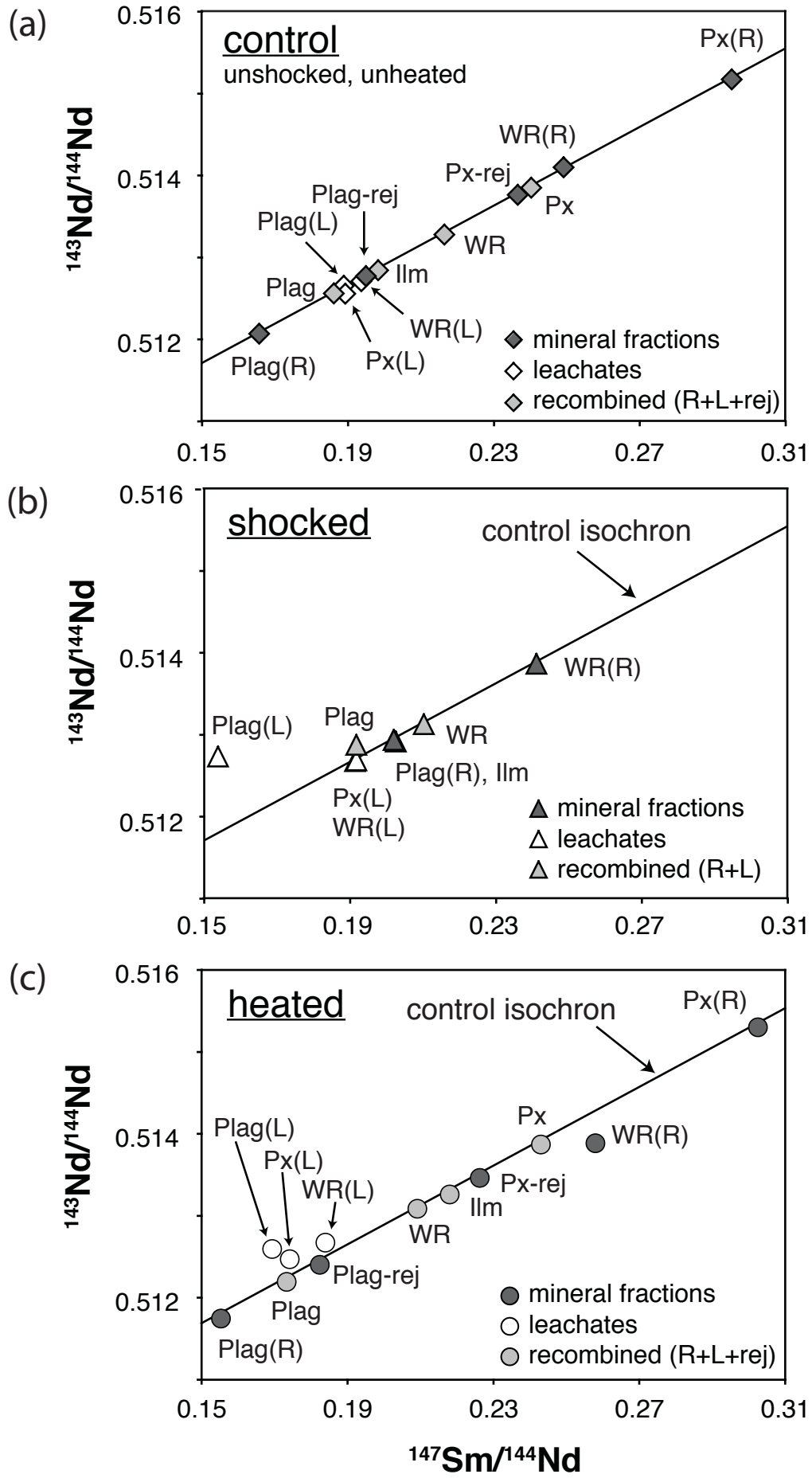
(a)
control
unshocked, unheated
Px(R)
WR(R)
Px-rej
Px
Plag-rej
Plag(L)
WR
Ilm
Plag
WR(L)
Plag(R)
Px(L)
mineral fractions
leachates
recombined (R+L+rej)
(b)
shocked
control isochron
WR(R)
Plag(L)
Plag
WR
Plag(R), Ilm
Px(L)
WR(L)
mineral fractions
leachates
recombined (R+L)
(c)
heated
control isochron
Px(R)
Px
WR(R)
Plag(L)
Px(L)
WR(L)
Px-rej
Ilm
WR
Plag-rej
Plag
Plag(R)
mineral fractions
leachates
recombined (R+L+rej)
0.516
0.514
0.512
0.15
0.19
0.23
0.27
0.31
143Nd/144Nd
147Sm/144Nd

Figure 2

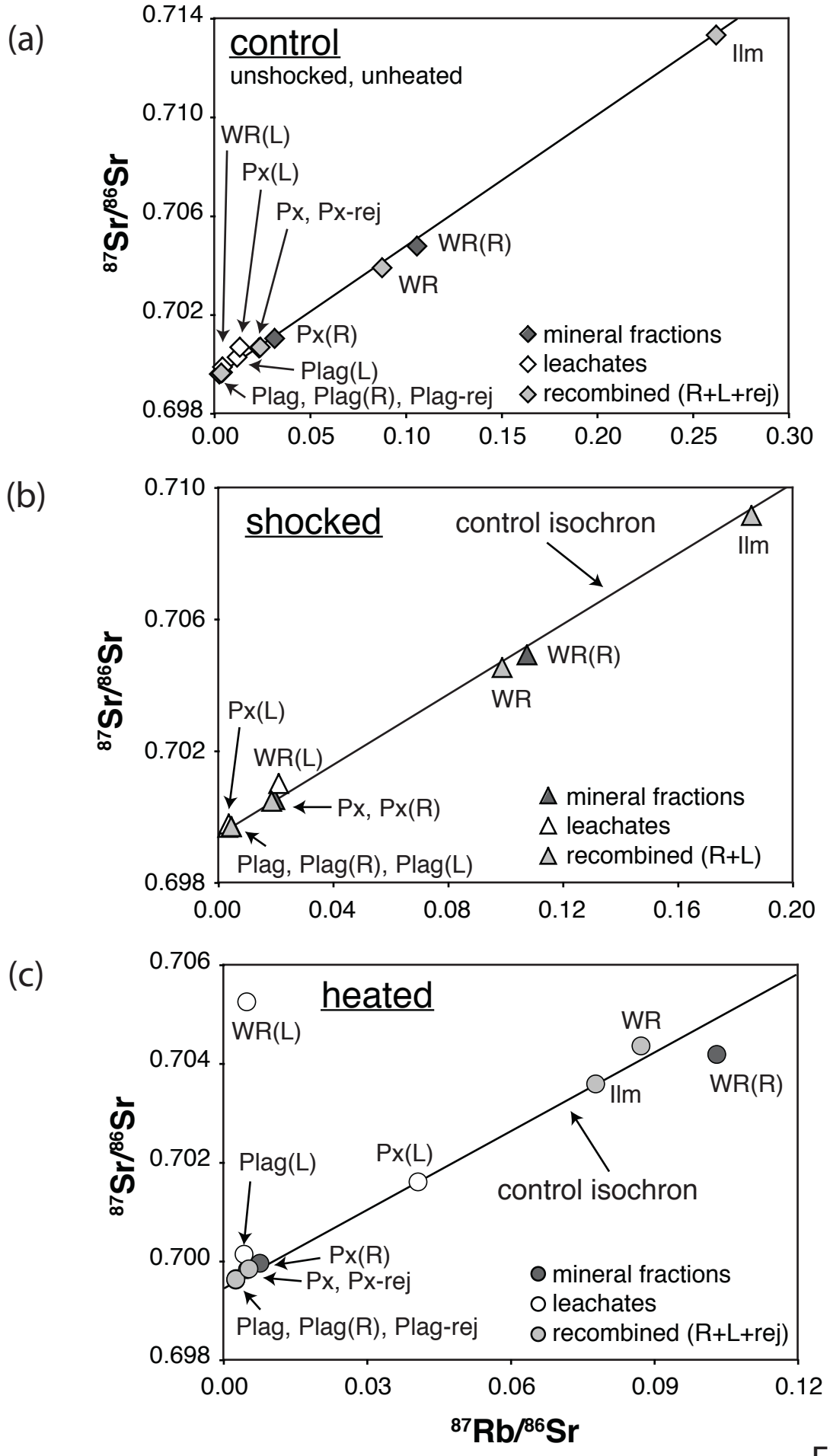
(a)
control
unshocked, unheated
Ilm
WR(L)
Px(L)
Px, Px-rej
WR(R)
WR
Px(R)
Plag(L)
Plag, Plag(R), Plag-rej
mineral fractions
leachates
recombined (R+L+rej)
0.714
0.710
0.706
0.702
0.698
0.00
0.05
0.10
0.15
0.20
0.25
0.30
87Sr/86Sr
(b)
shocked
control isochron
Ilm
WR(R)
WR
Px(L)
WR(L)
Px, Px(R)
Plag, Plag(R), Plag(L)
mineral fractions
leachates
recombined (R+L)
0.710
0.706
0.702
0.698
0.00
0.04
0.08
0.12
0.16
0.20
87Sr/86Sr
(c)
heated
WR(L)
WR
Ilm
WR(R)
Plag(L)
Px(L)
control isochron
Px(R)
Px, Px-rej
Plag, Plag(R), Plag-rej
mineral fractions
leachates
recombined (R+L+rej)
0.706
0.704
0.702
0.700
0.698
0.00
0.03
0.06
0.09
0.12
87Sr/86Sr
87Rb/86Sr

Figure 3

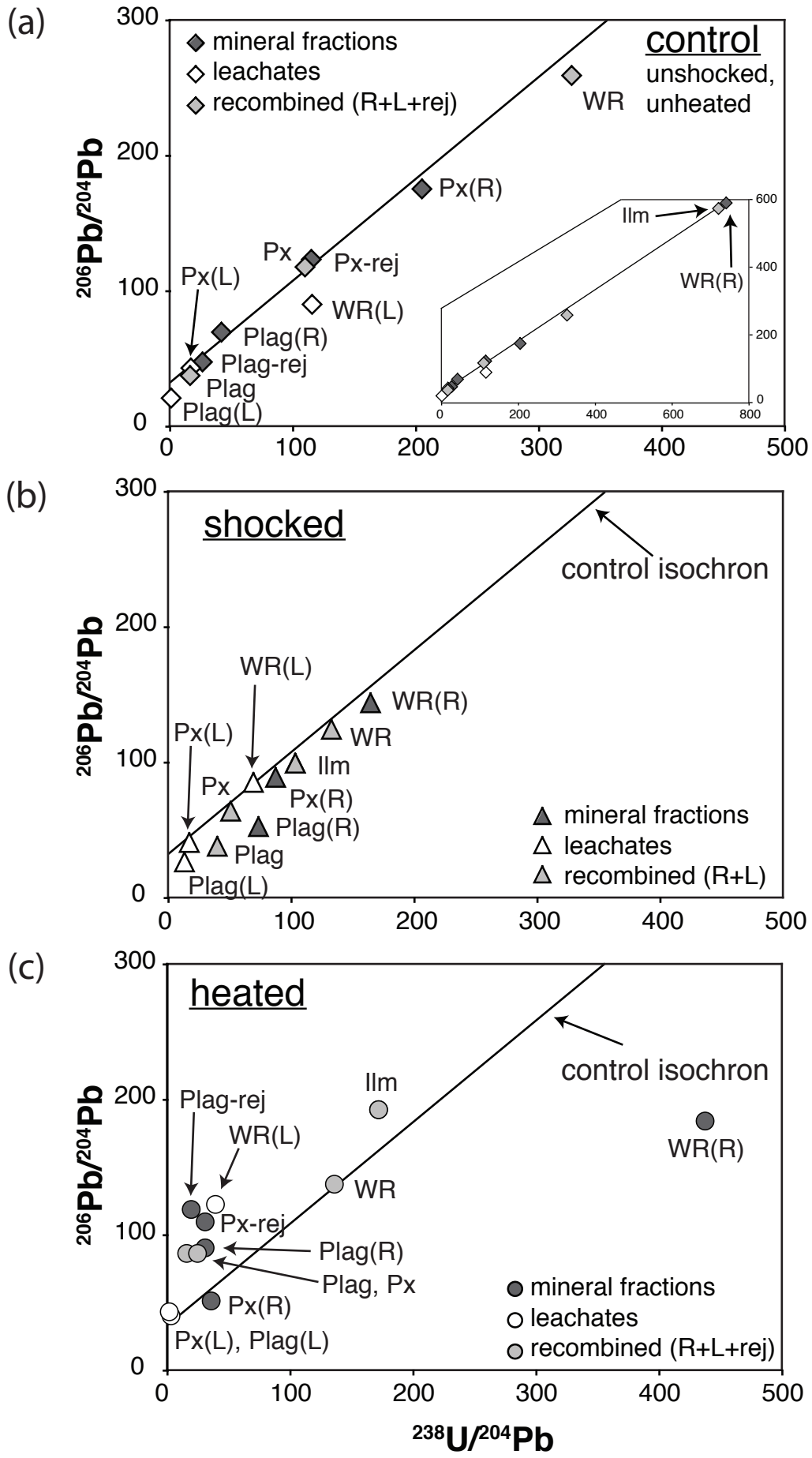
(a)
mineral fractions
leachates
recombined (R+L+rej)
control
unshocked,
unheated
WR
Px(R)
Px
Px-rej
Px(L)
WR(L)
Plag(R)
Plag-rej
Plag
Plag(L)
Ilm
WR(R)
(b)
shocked
control isochron
WR(L)
WR(R)
WR
Px(L)
Ilm
Px
Px(R)
Plag(R)
Plag
Plag(L)
mineral fractions
leachates
recombined (R+L)
(c)
heated
control isochron
Ilm
Plag-rej
WR(L)
WR(R)
WR
Px-rej
Plag(R)
Plag, Px
Px(R)
Px(L), Plag(L)
mineral fractions
leachates
recombined (R+L+rej)
206Pb/204Pb
238U/204Pb
0
100
200
300
400
500
600
800

Figure 4

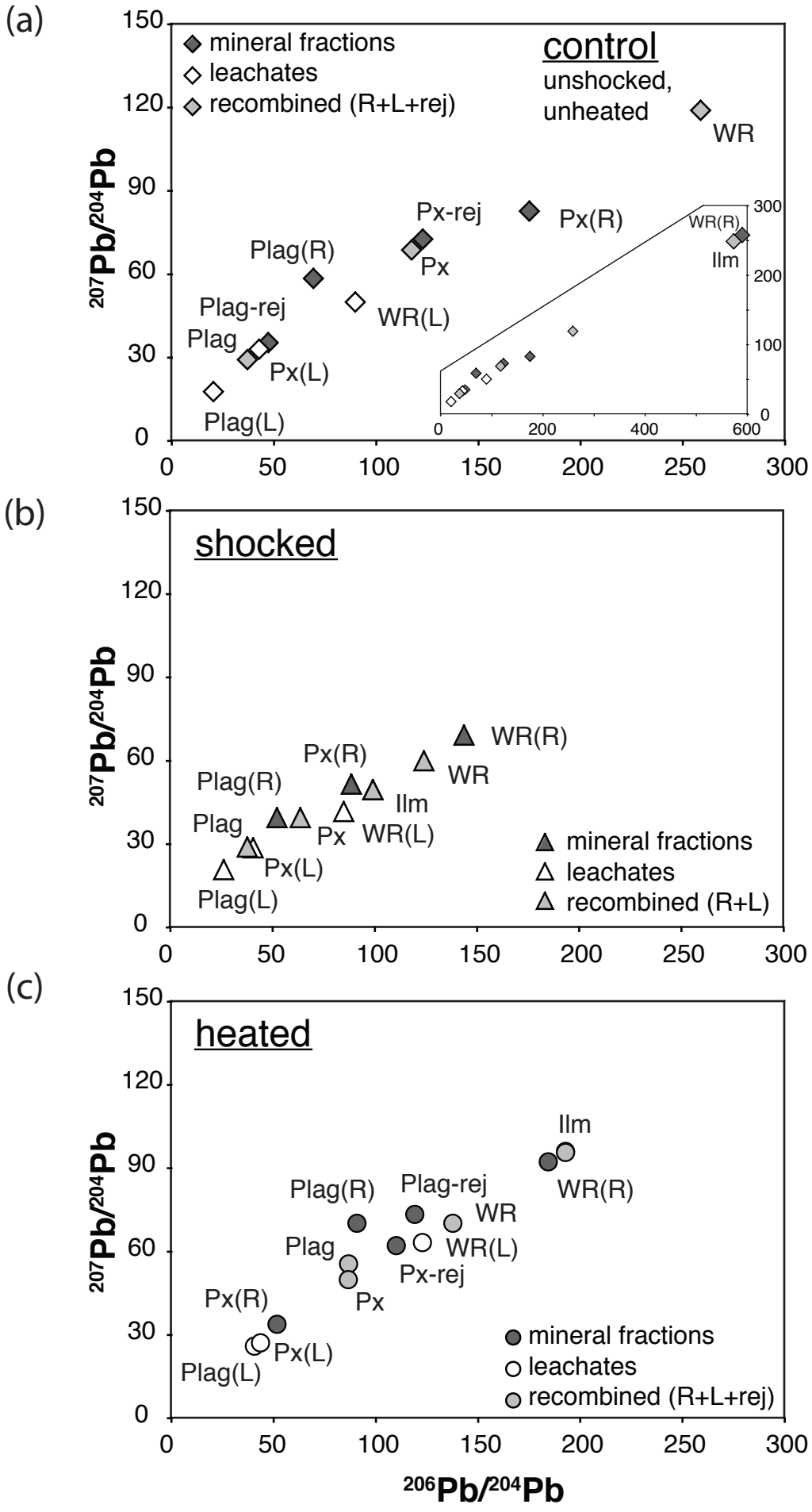
(a)
mineral fractions
leachates
recombined (R+L+rej)
control
unshocked,
unheated
WR
Px-rej
Px(R)
Plag(R)
Px
Plag-rej
WR(L)
Plag
Px(L)
Plag(L)
WR(R)
Ilm
(b)
shocked
WR(R)
Px(R)
WR
Plag(R)
Ilm
Plag
Px
WR(L)
Px(L)
Plag(L)
mineral fractions
leachates
recombined (R+L)
(c)
heated
Ilm
WR(R)
Plag(R)
Plag-rej
WR
Plag
WR(L)
Px-rej
Px
Px(R)
Px(L)
Plag(L)
mineral fractions
leachates
recombined (R+L+rej)
207Pb/204Pb
206Pb/204Pb

Figure 5

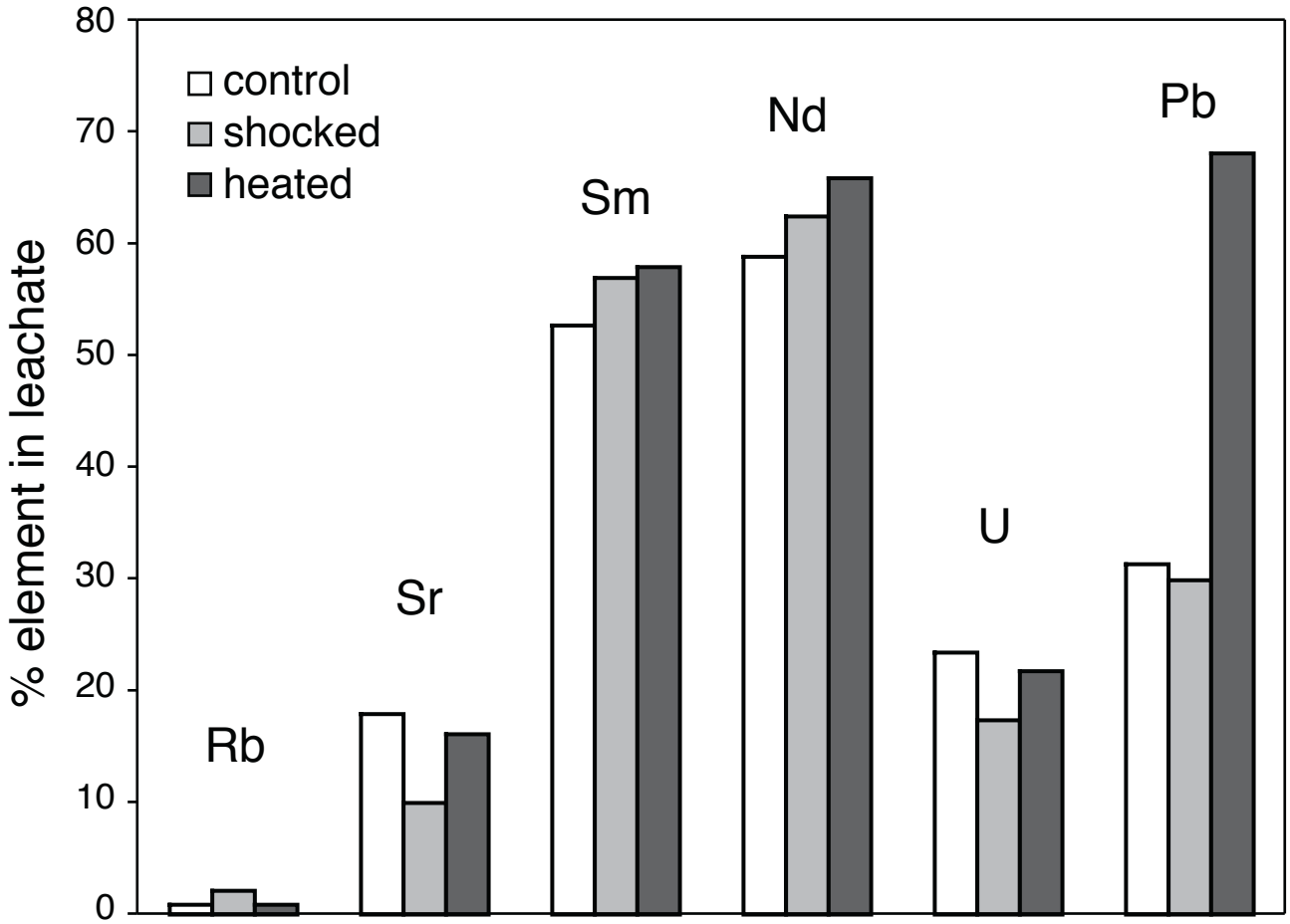
80
70
60
50
40
30
20
10
0
% element in leachate
control
shocked
heated
Rb
Sr
Sm
Nd
U
Pb

Figure 6

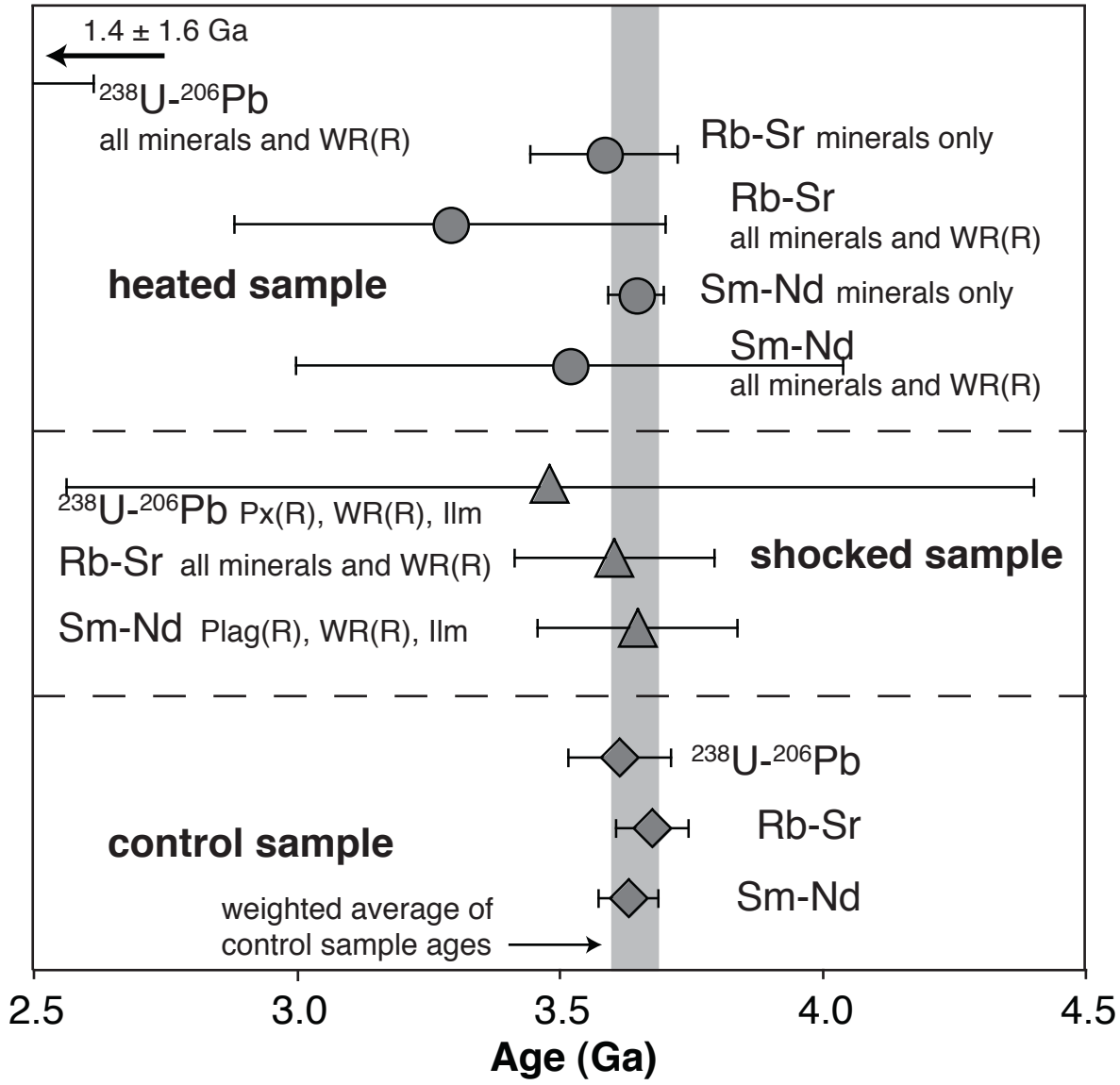
1.4 ± 1.6 Ga
238U-206Pb
all minerals and WR(R)
Rb-Sr minerals only
Rb-Sr
all minerals and WR(R)
heated sample
Sm-Nd minerals only
Sm-Nd
all minerals and WR(R)
238U-206Pb Px(R), WR(R), Ilm
Rb-Sr all minerals and WR(R)
shocked sample
Sm-Nd Plag(R), WR(R), Ilm
238U-206Pb
Rb-Sr
control sample
Sm-Nd
weighted average of
control sample ages
2.5
3.0
3.5
4.0
4.5
Age (Ga)

Figure 7

Table 1: Sm-Nd data

	wt. (mg)	Sm (ppm)	Sm (ng)	Nd (ppm)	Nd (ng)	$^{147}Sm/^{144}Nd$[a]	$^{143}Nd/^{144}Nd$[b]
Shocked sample							
Plag (R)	3.07	1.090	3.345	3.251	9.979	0.20267 ± 26	0.512913 ± 10
Plag (L)			0.7254		2.850	0.15388 ± 79	0.512728 ± 20
Px (L)			15.99		50.49	0.19147 ± 19	0.512672 ± 10
WR (R)	20.14	6.877	138.5	17.23	347.1	0.24121 ± 24	0.513860 ± 10
WR (L)			183.3		577.8	0.19184 ± 19	0.512682 ± 10
Ilm	28.00	32.72	916.1	97.88	2741	0.20209 ± 20	0.512930 ± 10
Heated sample							
Plag (R)	4.87	0.6173	3.006	2.405	11.71	0.15519 ± 19	0.511752 ± 10
Plag (L)			0.1991		0.7112	0.1692 ± 32	0.512602 ± 34
Plag-rej	7.81	0.905901	7.075	3.004	23.46	0.18228 ± 18	0.512410 ± 10
Px (R)	3.09	3.155	9.749	6.308	19.49	0.30235 ± 30	0.515305 ± 10
Px (L)			0.4872		1.693	0.1740 ± 14	0.512475 ± 23
Px-rej	11.32	2.063	23.35	5.515	62.42	0.22616 ± 23	0.513468 ± 10
WR (R)	28.42	7.284	207.0	17.08	485.5	0.25780 ± 26	0.513890 ± 10
WR (L)			285.4		938.4	0.18384 ± 18	0.512679 ± 10
Ilm	9.46	12.80	121.1	35.53	336.1	0.21788 ± 22	0.513268 ± 10
La Jolla (n = 5)[c]					10		0.511843 ± 41

Plag = plagioclase, Px = pyroxene, WR = whole rock, Ilm = ilmenite, (L) = HCl leachate, (R) = HCl-leached residue, rej = portion of mineral fraction rejected during hand-picking. All samples and standards run as NdO^+. The Px (R) fraction for the shocked sample failed to run on the mass spectrometer.

a. Error limits include a minimum uncertainty of 0.1% plus 50% of the blank correction for Sm and Nd added quadratically.

b. Normalized to $^{146}Nd/^{144}Nd = 0.7219$. Uncertainties are $2\sigma_m$ calculated from the measured isotope ratios. $2\sigma_m = [\Sigma(m_i-\mu)^2/(n(n-1))]^{1/2}$ for n ratio measurements m_i with mean value μ.

c. Error limits are $2\sigma_p$. $2\sigma_p = [\Sigma(M_i-\pi)^2/(N-1)]^{1/2}$ for N measurements M_i with mean value π. Isochrons are calculated using either $2\sigma_p$ (from standard runs) or $2\sigma_m$(from measured isotope ratios), whichever is larger.

Table 2: Rb-Sr data

	wt. (mg)	Rb (ppm)	Rb (ng)	Sr (ppm)	Sr (ng)	$^{87}Rb/^{86}Sr^{a}$	$^{87}Sr/^{86}Sr^{b}$
Shocked sample							
Plag (R)	3.07	0.6588	2.022	418.3	1284	0.004557 ± 46	0.699693 ± 10
Plag (L)			0.06841		59.29	0.003339 ± 15	0.699673 ± 10
Px (R)	8.77	1.665	14.60	244.3	2143	0.01971 ± 20	0.700515 ± 10
Px (L)			0.1973		157.2	0.003632 ± 55	0.699777 ± 11
WR (R)	20.14	5.794	116.7	155.9	3140	0.1075 ± 11	0.704917 ± 10
WR (L)			2.539		349.2	0.02104 ± 21	0.701004 ± 11
Ilm	28.00	11.78	329.8	183.6	5140	0.1857 ± 19	0.709146 ± 10
Heated sample							
Plag (R)	4.87	0.428705	2.088	501.2	2441	0.002475 ± 25	0.699624 ± 10
Plag (L)			0.006371		4.373	0.0042 ± 20	0.700147 ± 11
Plag-rej	7.81	0.4024	3.143	461.8	3606	0.002521 ± 25	0.699652 ± 10
Px (R)	3.09	0.4501	1.391	173.2	535.2	0.007519 ± 75	0.699966 ± 10
Px (L)			0.039851		2.843	0.0406 ± 31	0.701613 ± 14
Px-rej	11.32	0.6752	7.644	396.7	4490	0.004926 ± 49	0.699834 ± 10
WR (R)	28.42	4.484	127.4	126.0	3580	0.1030 ± 10	0.704192 ± 10
WR (L)			1.132		688.1	0.004760 ± 48	0.705261 ± 10
Ilm	9.46	4.040	38.22	150.4	1423	0.07772 ± 78	0.703596 ± 10
NBS 987 (n = 7)[c]					500		0.710257 ± 30

Plag = plagioclase, Px = pyroxene, WR = whole rock, Ilm = ilmenite, (L) = HCl leachate, (R) = HCl-leached residue, rej = portion of mineral fraction rejected during hand-picking.

a. Error limits include a minimum uncertainty of 1% plus 50% of the blank correction for Rb and Sr added quadratically.

b. Normalized to $^{86}Sr/^{88}Sr = 0.1194$. Uncertainties are $2\sigma_m$ calculated from the measured isotope ratios. $2\sigma_m = [\Sigma(m_i-\mu)^2/(n(n-1))]^{1/2}$ for n ratio measurements m_i with mean value μ.

c. Error limits are $2\sigma_p$. $2\sigma_p = [\Sigma(M_i-\pi)^2/(N-1)]^{1/2}$ for N measurements M_i with mean value π. Isochrons are calculated using either $2\sigma_p$ (from standard runs) or $2\sigma_m$ (from measured isotope ratios), whichever is larger.

Table 3: U-Pb data

	wt. (mg)	U (ppm)	U (ng)	Pb (ppm)	Pb (ng)	$^{238}U/^{204}Pb^{a}$	$^{206}Pb/^{204}Pb^{b}$	$^{207}Pb/^{204}Pb^{b}$	$^{208}Pb/^{204}Pb^{b}$
Shocked sample									
Plag (R)	3.07	0.08755	0.2688	0.1624	0.4986	73.4 ± 3.8	52.43 ± 0.92	39.39 ± 0.67	64.96 ± 0.79
Plag (L)			0.06121		0.3742	13.4 ± 3.2	26.277 ± 0.097	20.692 ± 0.079	47.10 ± 0.15
Px (R)	8.77	0.1690	1.482	0.3894	3.415	87.43 ± 0.50	88.77 ± 0.26	51.50 ± 0.15	92.19 ± 0.27
Px (L)			0.3162		2.232	17.19 ± 0.15	40.763 ± 0.070	28.502 ± 0.055	70.13 ± 0.15
WR (R)	20.14	0.6890	13.88	1.262	25.42	164.78 ± 0.44	143.86 ± 0.25	69.13 ± 0.13	135.68 ± 0.29
WR (L)			2.922		10.30	69.33 ± 0.26	84.98 ± 0.15	41.609 ± 0.082	155.29 ± 0.36
Ilm	28.00	1.618	45.29	3.629	101.6	103.57 ± 0.19	99.301 ± 0.090	49.47 ± 0.061	119.30 ± 0.19
Heated sample									
Plag (R)	4.87	0.01432	0.069723	0.1087	0.5296	30.6 ± 3.0	90.7 ± 2.7	70.2 ± 2.1	107.2 ± 2.6
Plag (L)			0.013352		0.5048	2.9 ± 4.8	40.53 ± 0.23	25.95 ± 0.13	61.52 ± 0.30
Plag-rej	7.81	0.01533	0.1197	0.2281	1.782	19.3 ± 1.4	119.0 ± 1.4	73.42 ± 0.83	139.0 ± 1.5
Px (R)	3.09	0.03670	0.1134	0.1435	0.4436	35.6 ± 3.0	51.6 ± 1.3	33.83 ± 0.78	74.8 ± 1.7
Px (L)			0.01037		0.8401	1.45 ± 0.62	43.56 ± 0.15	27.18 ± 0.13	64.24 ± 0.24
Px-rej	11.32	0.05266	0.5962	0.4526	5.124	30.63 ± 0.25	109.94 ± 0.38	62.19 ± 0.22	131.76 ± 0.49
WR (R)	28.42	0.4715	13.40	0.4490	12.76	437.2 ± 4.4	184.36 ± 0.46	92.34 ± 0.25	204.60 ± 0.62
WR (L)			3.727		27.41	39.04 ± 0.24	122.70 ± 0.14	63.226 ± 0.092	145.65 ± 0.25
Ilm	9.46	0.4793	4.534	1.221	11.55	171.66 ± 0.69	192.71 ± 0.48	96.05 ± 0.26	216.79 ± 0.64
All Faraday runs: NBS 981 (n = 10)[c]					2		16.902 ± 0.034	15.440 ± 0.038	36.54 ± 0.11
Faraday-Daly runs: NBS 981 (n = 17)[c]					0.5-2		16.889 ± 0.081	15.436 ± 0.091	36.53 ± 0.24

Plag = plagioclase, Px = pyroxene, WR = whole rock, Ilm = ilmenite, (L) = HCl leachate, (R) = HCl-leached residue, rej = portion of mineral fraction rejected during hand-picking.

a. Error limits include a minimum uncertainty of 0.1% plus 50% of the blank correction for U and Pb added quadratically.

b. Uncertainties are $2\sigma_m$ calculated from the measured isotope ratios. $2\sigma_m = [\Sigma(m_i-\mu)^2/(n(n-1))]^{1/2}$ for n ratio measurements m_i with mean value μ.

c. Error limits are $2\sigma_p$. $2\sigma_p = [\Sigma(M_i-\pi)^2/(N-1)]^{1/2}$ for N measurements M_i with mean value π. The greater uncertainty on the Faraday-Daly standard runs reflects the added uncertainty from the Faraday-Daly gain calibration.

Isochrons are calculated using either $2\sigma_p$ (from standard runs) or $2\sigma_m$ (from measured isotope ratios), whichever is larger.

Table 4: Ages determined from control, shocked and heated samples

	age (Ma)	*initial isotopic composition*	*fractions used in age calculation*
control sample			
Sm-Nd	3633 ± 57	ε_{Nd} = +3.2 ± 0.4	all minerals and WR(R)
Rb-Sr	3678 ± 69	$^{87}Sr/^{86}Sr$ = 0.69941 ± 7	all minerals and WR(R)
^{238}U-^{206}Pb	3616 ± 98	$^{206}Pb/^{204}Pb$ = 31 ± 11	all minerals and WR(R)
shocked sample			
Sm-Nd	3650 ± 190	ε_{Nd} = +2.77 ± 0.64	Plag(R), WR(R), Ilm
Rb-Sr	3606 ± 190	$^{87}Sr/^{86}Sr$ = 0.69945 ± 29	all minerals and WR(R)
Rb-Sr	3609 ± 140	$^{87}Sr/^{86}Sr$ = 0.69946 ± 18	recombined fractions + Ilm
^{238}U-^{206}Pb	3484 ± 630	$^{206}Pb/^{204}Pb$ = 26 ± 21	Px(R), WR(R), Ilm
heated sample			
Sm-Nd	3521 ± 520	ε_{Nd} = +1.6 ± 3.7	all minerals and WR(R)
Sm-Nd	3647 ± 53	ε_{Nd} = +2.38 ± 0.37	all minerals
Sm-Nd	3632 ± 120	ε_{Nd} = +2.57 ± 0.45	recombined fractions + Ilm
Rb-Sr	3293 ± 410	$^{87}Sr/^{86}Sr$ = 0.69958 ± 32	all minerals and WR(R)
Rb-Sr	3586 ± 140	$^{87}Sr/^{86}Sr$ = 0.699540 ± 68	all minerals
Rb-Sr	3758 ±490	$^{87}Sr/^{86}Sr$ = 0.69953 ± 42	recombined fractions + Ilm
^{238}U-^{206}Pb	1416 ± 1600	$^{206}Pb/^{204}Pb$ = 95 ± 59	all minerals and WR(R)
^{238}U-^{206}Pb	3108 ± 2100	$^{206}Pb/^{204}Pb$ = 72 ± 59	recombined fractions + Ilm